Original Article
Food Science and Technology

ISSN 0101-2061 (Print)
ISSN 1678-457X (Online)

DOI: https://doi.org/10.1590/fst.003523

Structural characterization of a polysaccharide from *Lyophyllum decastes* with MAPK-mediated immune regulation ability in mice

Yisi MA[1,2*], Qi WANG[1*]

Abstract

Lyophyllum decastes is a common macrofungi for both medicinal and economic value, and its polysaccharide has excellent development potential as a new immune regulator. In the present study, the bioactive component polysaccharide of *L decastes* was extracted, and its chain structure was characterized in detail by Fourier transform infrared (FT-IR) spectroscopy, high-performance gel-permeation chromatography (HP-GPC), and gas chromatography–mass spectrometry (GC–MS). LDP-W had a molecular weight of 2.12×10^4 Da, highly branched β type pyranose. At the same time, it exhibited potential immunomodulatory activity, which can modulate the numbers of CD3+, CD4+, CD8+ and CD19+ cells in the spleen; optimize the CD4+/CD8+ ratio; promoted T and B lymphocyte proliferation and it can elevate the levels of IL-2, IL-6, IFN-γ and TNF-α in immunosuppressed mice by influencing the phosphorylation of MAPK signaling-related proteins. These studies fill the gap in the immune regulation mechanism of *L decastes* polysaccharide, providing a theoretical basis for the potential application of LDP-W as immunomodulatory drugs or functional foods.

Keywords: *Lyophyllum decastes*; polysaccharides; structural elucidation; immunomodulatory activity.

Practical Application: A polysaccharide with the ability to regulate immunity.

1 Introduction

Malignant tumor is a kind of common disease that seriously threatens human health and life safety, and chemotherapy is still one of the main treatment methods (Gao & Zhao, 2022). However, chemotherapy drugs will destroy the patient's immune barrier while destroying tumor cells, leading to other diseases, such as bone marrow suppression, liver damage, immune organ atrophy, immune cell depletion, and other diseases (Fatmi et al., 2022). In addition, clinical diagnosis shows that patients receiving long-term chemotherapy will experience immunosuppression, leading to inhibition or even loss of the body's ability to respond to antigens (Yan et al., 2014). Therefore, it is a common treatment method to give appropriate immune modulator to alleviate immunosuppression during treatment to improve the immune ability of chemotherapy patients (Jiang et al., 2010).

Polysaccharides are an important class of biological macromolecules present in all living organisms (El-Naggar et al., 2020).They perform various biological functions, including immunomodulatory (Ramberg et al., 2010), antitumor (Meng et al., 2017), antidiabetic (Ganesan & Xu, 2019), anticoagulant (Hu et al., 2020), antiviral (Chaisuwan et al., 2021) and antioxidant activities (Wang & Liu, 2020). It can accelerate, enhance, or prolong the immune response affected by the host immune status, administration route and application dose (Han et al., 2022). Several studies have shown that β-polysaccharides with a complex structure, such as dextran, can interact with various receptors on the surface of effector cells (macrophages, monocytes, neutrophils, NK cells, dendritic cells, T cells and B cells) (Zheng et al., 2017). The receptor binds to and activates various effector cells, thereby increasing the secretion of proinflammatory chemokines and cytokines such as tumor necrosis factor-α (TNF-α), interleukin-1β (IL-1β), IL-6, IL-8, IL-12, interferon-γ (IFN-γ) and IFN-β (Hassan et al., 2021). Several studies have reported that fungal polysaccharides have a high potential for use as a natural immune regulator (Guo et al., 2021).

In Asian countries, *Lyophyllum decastes* is a delicious and popular dual-purpose fungus used in medicine and food. It has a pleasant taste and exhibits various pharmacological activities, including lowering blood lipid (Ukawa et al., 2002), radioprotective (Nakamura et al., 2007), antidiabetic (Miura et al., 2002), antitumor (Ukawa et al., 2000), thrombolytic (Ukawa et al., 2001), alleviating acute liver injury (Zhang et al., 2022) and bacteriostatic effects (Arase et al., 2013). However, despite these beneficial health effects, there is a lack of comprehensive research on the immunoregulation activity of the fruiting body polysaccharides of *L. decastes*.

The isolation, characterization and determination of the immunomodulatory activity of the tested LDP-W are described in the following sections. These results provide a strong foundation to conduct further investigations on the fruiting bodies of *L. decastes*.

2 Materials and methods

2.1 Experimental materials

The experimental material used in this study was the *L. decastes* fruiting body purchased from Shandong Fuhe Fungus

Received 13 Jan., 2023
Accepted 28 Feb., 2023
[1] *Engineering Research Center of Chinese Ministry of Education for Edible and Medicinal Fungi, Jilin Agricultural University, Changchun, China*
[2] *Biology Teaching and Research Group, Changchun Second Middle School, Changchun, China*
*Corresponding author: mayisi0001@gmail.com; qwang6306@hotmail.com

Technology Co., Ltd. (Tai Ping Zhen Xi Heng He Cun, Zoucheng City, Jining City, Shandong Province, China). The material was identified as *L. decastes* belonging to the order Agaricales, family Tricholomataceae, and genus *Lyophyllum* by the experimental group of Professor Wang Qi from the Engineering Research Center of Chinese Ministry of Education for Edible and Medicinal Fungi, Jilin Agricultural University. This fruiting body specimen has been deposited in the mycological specimen center of Jilin Agricultural University.

2.2 Experimental animals

Fifty BALB/c female mice (Specific pathogen free) aged 7-8 weeks and weighing 18-22 g was obtained from Beijing Huafukang biotechnology limited company (License number: SCXK 2019-0008). The following feeding conditions were maintained: temperature, 20 °C ± 2 °C; humidity, 50-60%. All animals were kept in a pathogen-free environment and ad lib fed. The procedures for care and use of animals were approved by the Ethics Committee of Jilin Agricultural University (2021-06-29-001), and all animal experimentation were in line with the ARRIVE guidelines.

2.3 Experimental reagents

The antigen repair solution and antibodies were purchased from eBioscience Company (Beijintg, China). Monosaccharide standards were obtained from Sigma-Aldrich (Shanghai, China). Western blotting (WB) assay-related experimental reagents were provided by Servicebio (Wuhan, China). The other chemicals and reagents were of analytical grade and were provided by Beijing Chemical Industry Group Co., Ltd (Beijintg, China). DEAE-52 cellulose was purchased from GE Whatman (Shanghai, China).

2.4 Extraction of polysaccharide from L. decastes

Five hundred grams of the fruiting body was weighed, dried, and crushed. The crushed material was then passed through a 100-mesh sieve. After treatment with a high-speed blender (Westinghouse, WFB-HS0466, USA) for 10 min for disrupting the cell wall, the dry powder of the fruiting body was obtained. Distilled water was added to the dry powder at the ratio of 1:40 (material to liquid), and the dry powder was subjected to extraction in a 70 °C water bath for 3 h. The process was repeated twice; the extract was combined and concentrate to one-third of the original volume. Add 95% ethanol to the concentrated solution until the final volume of the solution reached 85% (v/v) and crude polysaccharide was obtained from the precipitate. The crude polysaccharide was deproteinized using Sevag reagent and then filtered through a 0.45-μm membrane filter and finally obtained LDP (Yun et al., 2022).

2.5 Purification of LDP

LDP was loaded on a DEAE-52 chromatographic column (Φ2.6 cm×20 cm) and eluted with NaCl solutions of varying concentrations at the flow rate of 1 mL/min. The fraction of the eluate with the highest yield and the highest activity was collected, and the purified polysaccharide component was obtained through dialysis and freeze-drying. Next, 20 mg of the eluted polysaccharide was accurately weighed and dissolved in 4 mL deionized water. The mixture was then subjected to chromatography by using a Sephacryl S-300 gel column (Φ 2.6 cm × 100 cm), with the flow rate of 0.5 mL/min. The fractions were acquired by an automatic fractionation collector (Luxi Analytical Instrument Co., Ltd., automatic partial collector SBS-160, Shanghai); the procedure was performed at the speed of 10 min/tube (Cui et al., 2023). The polysaccharide content in each tube was determined by the phenol-sulfuric acid method, and the elution curve was then drawn. The absorbance value was read at 490 nm. The active ingredient (LDP-W) was collected, dialyzed, concentrated, freeze-dried, and preserved.

2.6 Analysis of LDP-W composition and relative molecular mass

The total carbohydrate content of LDP-W was measured by the phenol-sulfuric acid method. The protein content was determined by Coomassie Brilliant Blue staining. The molecular weight of LDP-W was estimated using an evaporative light scattering detector (Agilent Technologies Co. Ltd., 1260 Infinity ELSD, USA). The assay was performed on a TSK-gel G-3000PWXL column (Φ 7.8 mm × 300 mm) with distilled water as the mobile phase; the flow rate was 0.5 mL/min, the column temperature was 35 °C, and the injection volume was 10 μL. The sample was tested under these detection conditions, and the results were calculated with GPC software.

2.7 Determination of monosaccharide composition of LDP-W

The monosaccharide composition of LDP-W was determined using a method similar to that of McConnell & Antoniewicz (2016), with slight modifications. ddH_2O was used as mobile phase A, 100 mmol/L NaOH solution as mobile phase B, and 100 mmol/L NaOH/200 mmol/L NaAc as mobile phase C. The flow rate was set to 0.5 mL/min, and the samples were detected on a PA20 ion chromatographic column with Dionex™ and CarboPac™. The measurement data were analyzed by chromeleon software (version 7.2).

2.8 Fourier transform infrared spectroscopy

LDP-W (2.0% ± 0.5% mg) was dried sufficiently and mixed with 100 mg of spectroscopic-grade KBr powder. The mixture was milled properly and then pressed into a 1-mm-thick slice with a hydraulic press. The Fourier transform infrared (FT-IR) spectra of the pellet were then recorded in the range of 500-4000 cm^{-1} (Thermo Fisher Scientific, Nicolet IS5, USA).

2.9 Methylation analysis

Methylation analysis of LDP-W was performed to determine the nature of the glycosidic bonds according to the reported method (Ji et al., 2018).

Chromatographic conditions: The test conditions were as follows: carrier gas: high-purity helium; flow rate: 1.0 mL/min; injection volume: 1 μL. The split ratio was 10:1, and the temperature of the injection port was 260 °C; the initial temperature of the column temperature box was 140 °C, and it was maintained for

2 min. The program temperature was set to increase at the rate of 3 °C/min to 230 °C, and it was maintained for 3 min.

Mass spectrum conditions: The temperature of the injection port was set at 230 °C, and the temperature of the fourth stage rod was 150 °C. The full-scan mode (SCAN) was used for scanning, and the scanning quality range was 30-600 m/z (Shimadzu, GC-2014C, Shanghai).

2.10 NMR spectroscopy analysis

LDP-W (50 mg) was dissolved in 0.5 mL of deuterium oxide (D_20) and then freeze-dried. This procedure was repeated three times to fully exchange active hydrogen, and the mixture was finally dissolved in D_20 in an NMR tube. ^{1}H NMR and ^{13}C NMR spectra were recorded on an NMR apparatus (Bruker, Avance III 600, USA) at 600 MHz at 25 °C (Le et al., 2022).

2.11 Surface morphology observation

LDP-W was dissolved and diluted with deionized water, and the final concentration was 10 μg/mL. Next, 5 μL samples were added in a dropwise manner to mica flakes and then dried under natural environmental conditions. The microstructure of LDP-W was observed using an atomic force microscope (Bruker, Dimension FastScan, USA).

2.12 Grouping and administration methods

50 experimental mice with similar physiological conditions were randomly divided into five groups, 10 in each group: normal control group (NC), cyclophosphamide (CTX) control group (MC), CTX + LDP-W (200 mg/kg) group, CTX + LDP-W (100 mg/kg) group, and CTX + LDP-W (50 mg/kg) group. CTX was intraperitoneally injected into mice. Four groups of mice except NC group, each mouse were injected daily for 5 days at the dose of 80 mg/kg. The stomach of mice in four CTX administration groups were daily irrigated with the indicated dose of LDP-W, while the stomach of mice in the MC group was daily irrigated with the same amount of normal saline after treatment with CTX. All groups were treated continuously for 20 days.

2.13 Immune organ index

At 24 h after the last administration, mice in each group were weighed and sacrificed by cervical dislocation. The spleen was immediately separated, and the weight of each organ was recorded. The spleen index of mice was expressed as the ratio of the weight of the spleen (mg), respectively, to the weight of mice (g).

2.14 Detection of lymphocyte subsets

Three mice from each group were taken, and spleen lymphocytes were prepared into single cell suspension under sterile conditions. For this purpose, 100 μL cell suspension was taken in a 1.5 mL EP tube, and 10 μL monoclonal antibodies was added, with a blank control. The mixed cell suspension was placed at 4 °C and incubated in dark for 30 min. Subsequently, the mixed cell suspension was washed twice with precooled FACS. The suspension was centrifuged for 5 min at 4 °C and 1500 rpm for each washing, and the volume was replenished to 100 μL. After washing, flow cytometry was used for detection (Becton Dickinson, FACS Calibur, USA).

2.15 MTT assay for lymphocyte proliferation

Single cell suspension of mouse spleen lymphocytes was prepared for each group and seeded onto a 96-well cell culture plate, with the addition of 100 μL cell suspension to each well. Next, 100 μL RPMI-1640 complete culture medium containing PHA and LPS was added to each well. The cell culture plate was incubated at 40 °C under 5% CO_2 concentration and saturated humidity for 2 h, and 20 μL MTT solutions with a mass fraction of 5 mg/mL was then added to each well for 3 h. After incubation, the culture suspension was centrifuged at 1000 rpm for 10 min, and 150 μL DMSO was added to each well after discarding the supernatant; the mixture was shaken for 10 min, and the absorbance was measured at 590 nm (Thermo Fisher Scientific, Varioskan Flash, USA).

2.16 Cytokine detection

The levels of cytokines TNF-α, INF-γ, IL-6, and IL-2 in plasma were detected by ELISA. In accordance with the manufacturer's protocol, the absorbance was measured with a multifunction enzyme standard instrument (Thermo Fisher Scientific, Varioskan Flash, USA), and the contents of TNF-α, INF-γ, IL-6, and IL-2 were calculated according to the standard concentration curve.

2.17 WB assay

Mouse spleen cells were washed twice with PBS to prepare cell lysate homogenates for protein extraction. The protein concentration of each sample was quantified using the BCA protein assay kit. The PVDF membrane (Millipore, USA) used for protein transfer was activated with methanol before the actual transfer. The membrane with transferred proteins was then placed on a decolorizing shaker at room temperature and blocked with 5% skimmed milk (with 0.5% TBST) for 1 h. Subsequently, the membrane was incubated overnight with primary antibodies at 4 °C, followed by incubation with secondary antibodies. Electrochemiluminescence (ECL)-A and ECL-B were mixed in equal volumes and allowed to be in full contact with proteins for protein visualization. The gray values of the protein bands were quantified by the alpha program.

2.18 Statistical analysis

Unless otherwise stated, the data are expressed as mean ± standard deviation (SD) of triplicate determinations. All the data were analyzed using IBM SPSS 21.0 software. Analysis of variance (one-way ANOVA) was used for multiple comparisons between the control and test conditions. $P < 0.05$ was considered statistically significant.

3 Results and discussion

3.1 Isolation and purification of LDP

LDP was obtained by hot water extraction and ethanol precipitation, and the yield was 32.64%. The crude polysaccharide

was deproteinized with the Sevag reagent and dialyzed to remove small molecule impurities. The subsequent yield rate was 20.96% (the ratio of crude polysaccharide weight to the weight of powder of the *L. decastes* fruiting body). The extraction rate is higher than that of *Pleurotus ostreatus* polysaccharides and agaric polysaccharides, and similar to that of *Ganoderma lucidum* polysaccharides (Wang et al., 2022).

According to the basic chemical composition of LDP, the contents of polysaccharides, proteins, and uronic acid were 64.09%, 14.81%, and 0.08%, respectively. LDP was separated sequentially on a DEAE-52 chromatographic column, and three fractions were obtained: F1, F2, and F3 (Figure 1A). Fraction F1 was further purified on a Sephacryl S-300 gel chromatography column, and the corresponding positive peaks were collected, dialyzed, and freeze-dried to obtain purified LDP, which was named as LDP-W with a yield of 4.26% (Figure 1B).

3.2 Molecular weight and monosaccharide composition of LDP-W

LDP-W showed weak characteristic absorption at 280 and 260 nm, indicating that there was almost no nucleic acid or protein in LDP-W, as determined by UV spectrum analysis. In the same detection method, LDP-W showed a maximum absorption peak near 199 nm, which indicated the presence of polysaccharides (Qiu et al., 2022). HP-GPC assay of LDP-W showed a single and symmetrical peak in the chromatogram, indicating that LDP-W is a fraction with uniform polysaccharide composition. By using the standard curve equation, the molecular weight of LDP-W was calculated as 2.12×10^4 Da (Figure 1C). The retention time of the hydrolyzed derivative of LDP-W was compared with that of each monosaccharide standard, as shown in Figure 1D. The main monosaccharides constituting LDP-W were Glc, Fru, Gla, and Fuc. LDP-W also contained a small amount of Rib, Ara, and Man (Table 1).

3.3 Results of FTIR spectroscopy

According to the published data, different structures correspond to different absorption bands. The absorption bands between 3500 and 3100 cm^{-1} were attributed to the vibration of the hydroxyl groups (Tian et al., 2016). As shown in Figure 2A, the broad absorbance bands at 3416.60 cm^{-1} were formed by the stretching vibration of the O-H bond, which is also the characteristic absorption peak of polysaccharides (Kim et al., 2016). The absorption peak at 1644.47 cm^{-1} corresponded to the tensile vibration of the C-O group. The peaks at 1413.96 cm^{-1} were also ascribed to the stretching vibration of the C-H bond (Duan et al., 2020). The signals at 1200-1000 cm^{-1} were defined as the molecular fingerprint region of polysaccharides, wherein the band at 1076.81 cm^{-1} was the characteristic absorption band of the pyranose ring (Ji et al., 2020).

3.4 Methylation analysis of LDP-W

Methylation analysis is a crucial chemical analytical method for studying the structures of carbohydrate by GC–MS (Cheng et al.,

Table 1. Monosaccharide composition and percentage of LDP-W.

Sample	Monosaccharide composition (mol%)					
	Fuc	Ara	Gal	Glc	Man	Fru
LDP-W	2.969	0.803	6.964	73.548	9.804	1.519

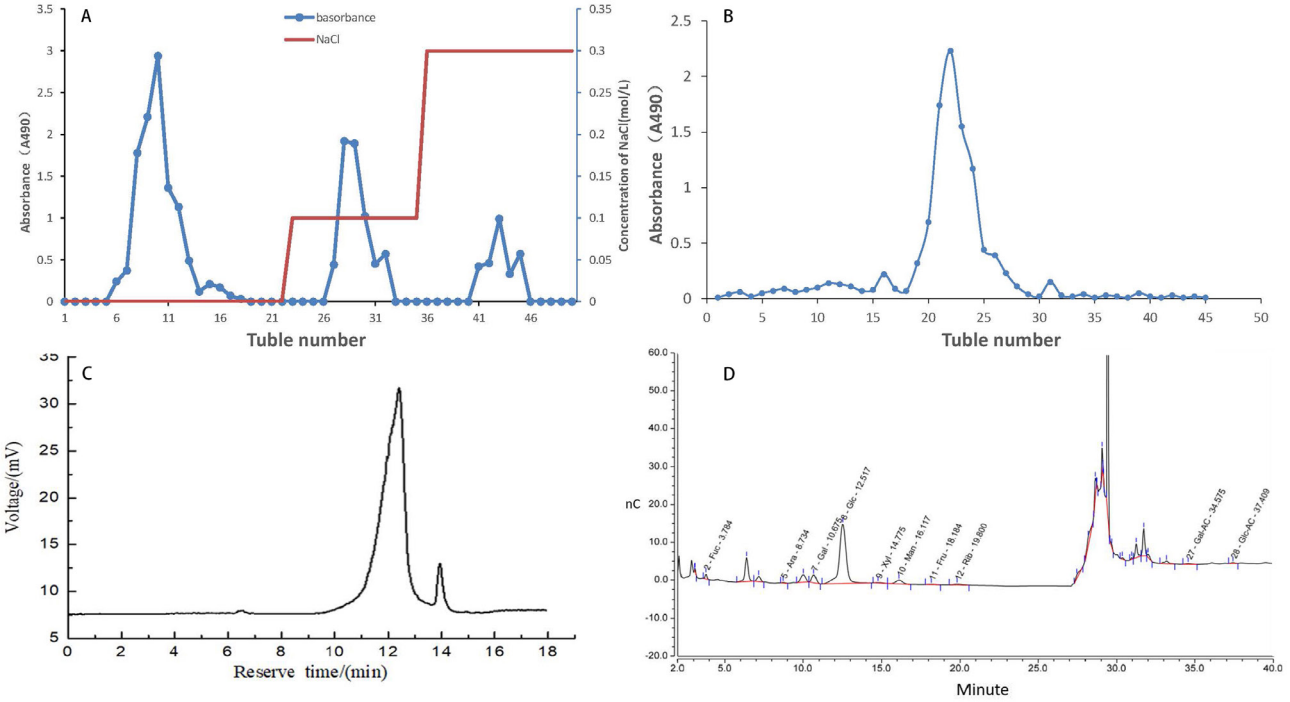

Figure 1. Chromatogram of LDP on DEAE-52 cellulose column (A), elution curves of LDP-W on Sephacryal S300 HR column (B), the high-performance liquid chromatogram of LDP-W (C), and analysis of monosaccharide composition of LDP-W (D).

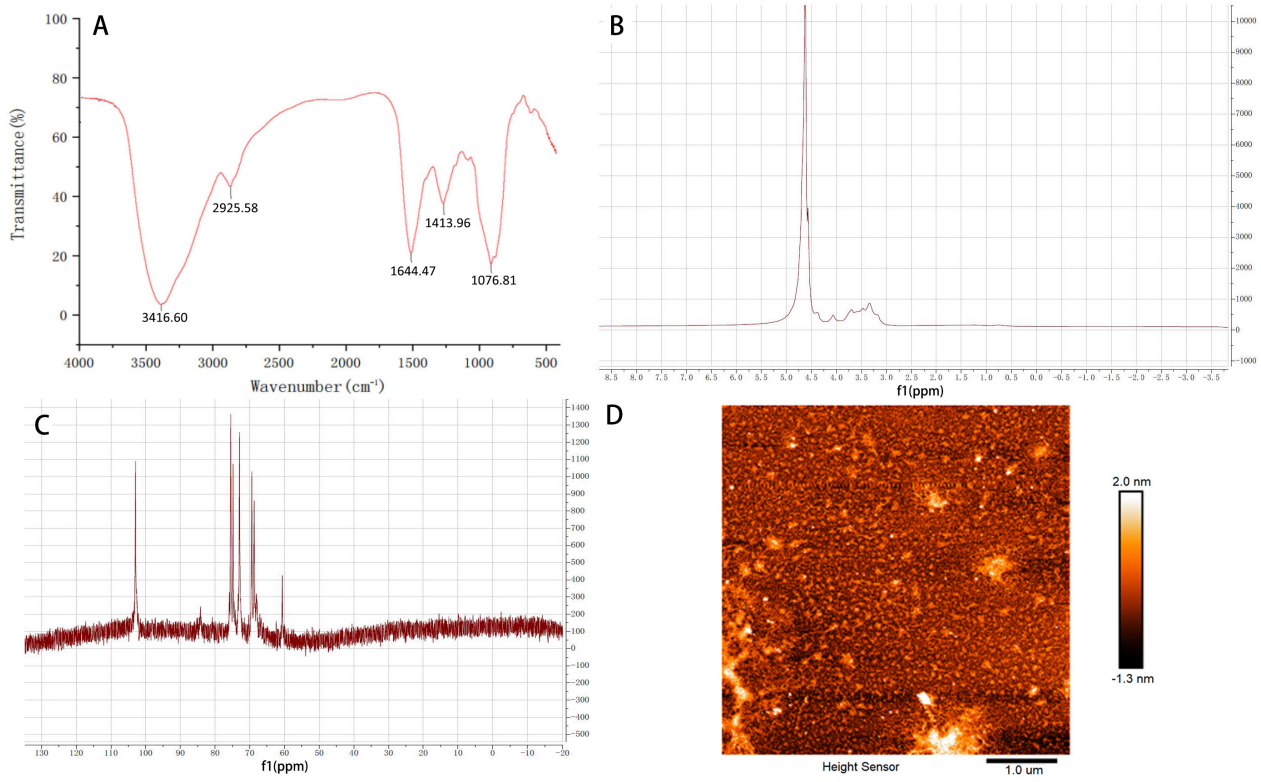

Figure 2. Chromatogram of LDP on DEAE-52 cellulose column (A), H NMR spectra of LDP-W (B), C NMR spectra of LDP-W (C), and atomic force microscopy of LDP-W (D).

Table 2. Methylation analysis results of LDP-W.

Connection mode	Name of derivative	Molecular weight	Mole ratio
t-Man(p)	1,5-di-O-acetyl-2,3,4,6-tetra-O-methyl mannitol	323	5.10
t-Glc(p)	1,5-di-O-acetyl-2,3,4,6-tetra-O-methyl glucitol	323	18.51
3-Glc(p)	1,3,5-tri-O-acetyl-2,4,6-tri-O-methyl glucitol	351	18.73
6-Glc(p)	1,5,6-tri-O-acetyl-2,3,4-tri-O-methyl glucitol	351	30.34
4-Glc(p)	1,4,5-tri-O-acetyl-2,3,6-tri-O-methyl glucitol	351	3.87
3,6-Glc(p)	1,3,5,6-tetra-O-acetyl-2,4-di-O-methyl glucitol	379	16.74
2,6-Gal(p)	1,2,5,6-tetra-O-acetyl-3,4-di-O-methyl galactitol	379	6.70

2020). This method is widely used to determine the type and relative content of glycosidic bonds of polysaccharides (Liang et al., 2019). The Complex Carbohydrate Research Center (CCRC) spectral database (University of Georgia, 2022) was used to determine the glycosidic bonds of sugar residues. The GC–MS analysis data of LDP-W are shown in Table 2. LDP-W contains seven types of methyl groups. The group with the largest proportion is 1,5,6-tri-O-acetyl-2,3,4-tri-O-methyl glucitol, followed by 1,3,5-tri-O-acetyl-2,4,6-tri-O-methyl glucitol, and 1,5-di-O-acetyl-2,3,4,6-tetra-O-methyl glucitol. This finding suggests that glucopyranose is 2,3,4-, 2,3,4,6-, and 2,4,6-bonded. Carboxymethylation at the C3 position is less likely to occur due to the steric hindrance effect at C3 and the intramolecular hydrogen bond between C2 and C3; this results in incomplete methylation. Thus, it can be concluded that LDP-W is composed of 1, 3, 6-Glcp; 1, 3, 4, 6-Glcp; and 2, 4, 6 Galp. Based on the peak area of monosaccharide residues, the results showed that the main repetitive structural unit of LDP-W was (2→4)-D-glucopyranose as the main chain and (2→6)-D-glucose as the side chain polysaccharide. These results are consistent with the monosaccharide composition of LDP-W. Moreover, according to the results of methylation analysis obtained in this study and the results of monosaccharide composition analysis obtained in previous studies, it can be deduced that the basic skeleton of LDP-W is formed through the glycosidic bonds of glucose (Ernst et al., 2023).

3.5 Results of NMR

NMR spectra analysis is an indispensable tool for analyzing the structure of polysaccharides, and it is one of the most accurate and efficient methods to analyze the structure of polysaccharides. Figure 2B is the hydrogen spectrum of LDP-W. The hydrogen spectrum signal is mainly concentrated in δ 3.0-5.0, among which δ 3.2-4.0 is the proton signal of the saccharide ring (Cai et al., 2018). In 1^H NMR, four anomeric proton signals were recorded, namely δ 4.67, δ 4.59, δ 4.41, and δ 4.08, which indicates that one repetitive unit of LDP-W contains four types of anomeric protons and that all belong to β-type pyranose. Signals at δ 4.11-3.18 were the overlapping hydrogen signals of H2–H6.

Similar to the hydrogen spectrum signal, the heteromeric carbon of sugar in the carbon spectrum was also located in a lower field of δ 95-110 (Liu et al., 2022). Figure 2C shows the one-dimensional carbon spectrum of LDP-W. The NMR spectra signals of LDP-W were mainly centered between δ 60 and δ 105. In the carbon spectrum, only one anomeric carbon signal peak was visible at δ 103.94 and was distributed in the anomeric carbon region δ 95-110. The chemical shifts of α-and β-glycosyl groups were located at δ 90-102 and δ 102-112, respectively (Song et al., 2019). Signals at δ 85.42-60.56 were the carbon signals of C2–C6. This further confirmed that LDP-W belongs to β-type pyranose.

3.6 Results of AFM analysis

AFM is a simple and accurate technique to observe the spatial conformation and appearance of macromolecules, and it can effectively characterize biopolymers at the sub-nanometer scale (Trache & Meininger, 2008). The surface morphology of LDP-W is shown in Figure 2D. Lumpy spherical aggregates of different sizes were observed by AFM, and the height was 0.10-13.45 nm. According to previous reports, the height of a monosaccharide chain is approximately 0.1-1.0 nm. Hence, it can be concluded that the aggregation reaction had occurred in the LDP-W molecule. Moreover, the LDP-W molecule was much larger than a single polysaccharide chain, thus indicating that the structural units of LDP-W were entangled with each other. Based on the above results, we speculate that not only entanglement or superposition of polymers but also a reduction in solvent volume occurred during the drying process, such that the sugar chains retained the polymers together through intermolecular and intramolecular hydrogen bond interactions.

3.7 Effect of LDP-W on the immune organ index

The immune organ index was calculated according to the weight of immune organs, and it was used to characterize the degree of damage and health status of the immune organs. One week after CTX administration, the spleen index and thymus index of immunosuppressed mice were significantly lower than those of the NC group ($P < 0.01$); this finding indicated that the experimental model had been successfully established.

Compared to the MC group, the immune organ index of each LDP-W administration group increased significantly with the increase in treatment duration, while the immune organ index of the NC group did not change significantly; this finding shows that the experimental results are reliable (Figure 3A). Compared to the other dose groups, the administration of LDP-W at a high dose significantly increased the immune organ index ($P < 0.05$), and the results were similar to those of the NC group. This finding confirmed that LDP-W treatment can significantly repair the damage of immune organs caused by CTX in mice, thus improving the immune ability of mice.

3.8 Effect of LDP-W on lymphocyte subsets

The results are shown in the Figure 3B and Figure 3C, compared to the NC group, the MC group showed lower percentage of CD3+, CD4+, CD8+, and CD19+ lymphocytes and lower ratio of CD4+/CD8+ T cells. The results for the low-dose group were slightly better than those for the MC group. The percentage of CD3+, CD4+, CD8+, and CD19+ lymphocytes and the ratio of CD4+/CD8+ T cells in the high-dose and middle-dose groups were significantly increased. The high-dose group also showed more significant upregulation of the ratio of CD4+/CD8+ T cells.

Lymphocytes play a very important role in the specific immune regulation of the body (Isakov& Altman, 1986). CD3 is a differentiation antigen specifically expressed by mature T cells. CD19 is a differentiation factor specifically expressed by mature B lymphocytes. The proportion of CD3 and CD19 in the MC group was significantly reduced as compared to that in the NC group, thus indicating that T and B lymphocyte activities in mice were inhibited by CTX administration. After intragastric administration of LDP-W, CD3 and CD19 levels in the serum of mice in each dose group were recovered to a certain extent, thus indicating that LDP-W can improve the immune ability of mice by enhancing the activities of T and B lymphocytes.

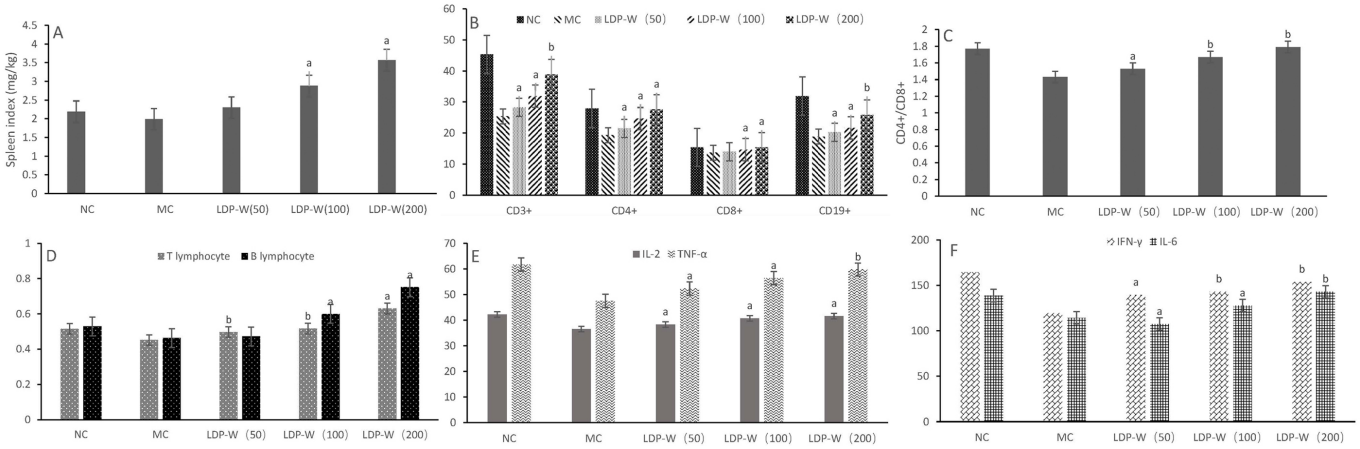

Figure 3. Effect of LDP-W on spleen index(A) (X ± s, n=10), effect of LDP-W on lymphocyte subsets (B) (C), effect of LDP-W on the value-added function of T and B lymphocytes (D), and effects of LDP-W on cytokines secreted by splenic lymphocytes (E) (F). A denotes significant differences ($p < 0.05$) compared with MC, b denotes significant differences ($p < 0.01$) compared with MC.

T lymphocyte-mediated cellular immunity plays an important role in body's immune defense and the elimination of infected cells (Bethge et al., 2010). T lymphoid cells are classified into CD4+ T cells and CD8+ T cells. The dynamic balance between these two subtypes is very important to maintain the stability of the immune status of the body (Serre et al., 2010). In the present study, we found that LDP-W can restore the proportion of CD4+ T cells and CD8+ T cells in the lymphoid cells of immunosuppressed mice, and LDP-W can increase the proportion of lymphocytes and reduce the proportion of cytotoxic T cells.

3.9 Effect of LDP-W on lymphocyte proliferation

Lymphocytes are an important part of the body's acquired immune system (Roszczyk et al., 2022). Activated T and B lymphocytes are critical components of the immune response of the body (Wei et al., 2022).The most apparent change in lymphocyte activation is cell division and proliferation (Almeida et al., 2015).Compared to the MC group, the number of T and B cells in blood of mice in each dose group increased significantly (Figure 3D).The results showed that LDP-W could directly stimulate the proliferation of splenic lymphocytes in immunosuppressed mice and then activate the mechanisms of cell division and differentiation, thereby improving the immune capacity of the body.

3.10 Effect of LDP-W on cytokines

Compared to the NC group, the release of the cytokines IL-2, IL-6, IFN-γ, and TNF-α was significantly reduced in the MC group. Furthermore, compared to the MC group, the amount of IL-2, IL-6, IFN-γ, and TNF-α secreted in mice serum in each dose administration group increased, and the amount of cytokine secretion dose-dependently increased with the increase in LDP-W administration concentration (Figure 3E,3F).

Cytokines promote the maturation and differentiation of lymphocytes and enhance the activities of toxic T lymphocytes and NK cells (Shardina et al., 2022). Cytokines produced by Th1 cells include IL-2, IL-12, IFN-γ, and TNF-α, which are mainly involved in mediating cellular immunity and activating macrophages and cytotoxic T lymphocytes (Khajepour et al., 2022). Th2 cells produce IL-4, IL-6, IL-10, and IL-13, whose main function is to enhance cellular immunity, promote the proliferation of B lymphocytes, and generate antibodies (Espinosa Gonzalez et al., 2022). IL-2 is a highly effective proliferation promoting factor for all T cell subtypes, and it functions by promoting G1 cell cycle (Jenkinson et al., 1987). In addition to affecting T cells, IL-2 also affects NK cells, LAK cells, B cells, macrophages, and other cells (Cluff et al., 2022). Therefore, the IL-2 production level is an important parameter to evaluate immune function. IFN-γ has a wide range of immune regulation capabilities; for example, it can activate macrophages and enhance their phagocytosis as well as increase NK cell activity and enhance their antibacterial and antitumor effects (Cao et al., 2013). IFN-γ can also improve the ability of anti-lymphocyte presentation (Chen et al., 2015). The present study showed that LDP-W stimulation leads to higher levels of IL-2 and IFN-γ. IL-6 is a Th2-type cytokine that plays an important role in promoting cell differentiation to Th2 (Eissa et al., 2022). The results showed that LDP-W could significantly enhance the secretion of IL-6. Thus, these results indicate that PSG-1 can simultaneously activate Th1 and Th2 cells.

3.11 Effect of LDP-W on the MAPK signal transduction pathway in splenic cells of immunosuppressed mice

Compared to the blank control group, the phosphorylation levels of P38, ERK, and JNK proteins in mouse spleen cells were decreased after CTX treatment. Furthermore, compared to the MC group, the phosphorylation levels of P38, ERK, and JNK proteins in all treated groups were relatively increased. The medium-dose group showed a significant increase in the protein phosphorylation level of JNK, and the high-dose group showed a significant increase in the protein phosphorylation level of ERK (Figure 4).

The MAPK pathway is a common junction pathway of cell proliferation, stress response, inflammation, differentiation, transformation, apoptosis, and other signal transduction pathways (Roberts et al., 2000). It is also an important pathway of immune-related signal transduction (Mohammed et al., 2020).

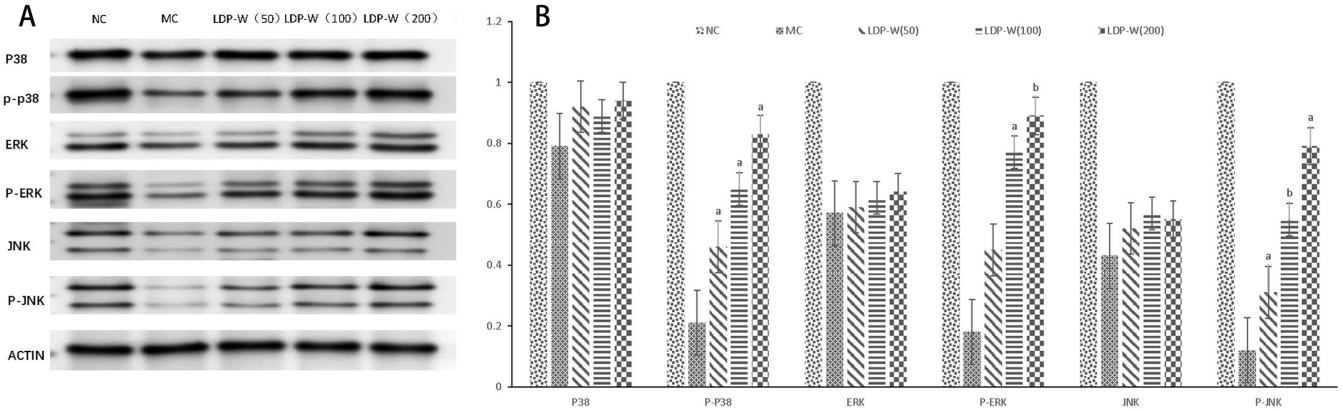

Figure 4. Effects of LDP-W on the phosphorylation of MAPK signaling pathway proteins in spleen cells (A), effect of LDP-W on the relative content of MAPK signaling pathway protein in spleen cells (B). A denotes significant differences ($p < 0.05$) compared with MC, b denotes significant differences ($p < 0.01$) compared with MC.

MAPK is an important protein that transmits information from the cell surface to the nucleus. It is expressed in all eukaryotic cells (Yin et al., 2021). The main role of MAPK is to receive extracellular signal stimuli and to amplify and transmit the stimulus signal cascade to the cell. This signaling pathway plays a critical role in the cell signal transduction pathway (Zhang et al., 2018). The MAPK family members are involved in three signaling pathways (P38, ERK1/2, and JNK pathways) (Cano& Mahadevan, 1995). ERK activation was considered to be related to the activity of immune cells; in particular, when macrophages are activated, ERK can increase the production of proinflammatory cytokines (Raman et al., 2007). P38 plays a particularly important role in the expression of TNF-a (Ito et al., 2006). JNK is ubiquitous in the body and plays an important role in immune regulation. After activation it can change the corresponding gene expression and affect the immune response of the body (Cargnello & Roux, 2011). These data confirm that LDP-W can affect the phosphorylation of P38, JNK, and ERK proteins in a dose-dependent manner, thus regulating MAPK-related signaling pathways.

4 Conclusion

In present study, the extraction, purification, characterization and immunomodulatory activity of polysaccharide from *L. decastes* were investigated. LDP-W is the main component, and describes their structure and immunoregulatory activity. LDP-W is a β pyran-type glucan with molecular weight of 2.12×10^4 Da. Additionally, LDP-W also shows a strong immunoregulatory effect, by activating the MAPK signal pathway, producing more cytokines, and regulating the number and proportion of immune cells. According to all these findings, LDP-W shows immunomodulatory effect, and can alleviate some side effects caused by the chemotherapeutic drug CTX, thus improving the survival of mice. It is expected that this research and the subsequent studies will help to improve the immune status of immunocompromised and immunosuppressed patients and reduce the side effects of chemotherapeutic drugs which might have positive effects on the production of functional foods and medications.

References

Almeida, V. C., Dupré, L., Guipouy, D., & Vasconcelos, Z. (2015). Signal integration during T lymphocyte activation and function: lessons from the Wiskott–Aldrich syndrome. *Frontiers in Immunology*, 6, 47. http://dx.doi.org/10.3389/fimmu.2015.00047. PMid:25709608.

Arase, S., Kondo, Y., Yanira, R., Jaco, R., Otani, H., Ueno, M., & Ichi, K. J. (2013). Suppression of rice blast disease by autoclaved water extract from the spent mushroom substrate of *Lyophyllum decastes*. *Mushroom Science and Biotechnology*, 21(2), 79-83. http://dx.doi.org/10.24465/msb.21.2_79.

Bethge, W. A., Faul, C., Bornhäuser, M., Stuhler, G., Beelen, D. W., Lang, P., Stelljes, M., Vogel, W., Hägele, M., Handgretinger, R., & Kanz, L. (2010). Haploidentical allogeneic hematopoietic cell transplantation in adults using CD3/CD19 depletion and reduced intensity conditioning: an update. *Blood Cells, Molecules & Diseases*, 40(1), 13-19. http://dx.doi.org/10.1016/j.bcmd.2007.07.001. PMid:17869547.

Cai, L. L., Zou, S. S., Liang, D. P., & Luan, L. B. (2018). Structural characterization, antioxidant and hepatoprotective activities of polysaccharides from *Sophorae Tonkinensis* Radix. *Carbohydrate Polymers*, 184, 354-365. http://dx.doi.org/10.1016/j.carbpol.2017.12.083. PMid:29352929.

Cano, E., & Mahadevan, L. C. (1995). Parallel signal processing among mammalian MAPKs. *Trends in Biochemical Sciences*, 20(3), 117-122. http://dx.doi.org/10.1016/S0968-0004(00)88978-1. PMid:7709430.

Cao, Z. H., Yin, W. D., Zheng, Q. Y., Feng, S. L., Xu, G. L., & Zhang, K. Q. (2013). Caspase-3 is involved in IFN-γ- and TNF-α-mediated MIN6 cells apoptosis via NF-κB/Bcl-2 pathway. *Cell Biochemistry and Biophysics*, 67(3), 1239-1248. http://dx.doi.org/10.1007/s12013-013-9642-4. PMid:23695786.

Cargnello, M., & Roux, P. P. (2011). Activation and function of the MAPKs and their substrates, the MAPK-activated protein kinases. *Microbiology and Molecular Biology Reviews*, 75(1), 50-83. http://dx.doi.org/10.1128/MMBR.00031-10. PMid:21372320.

Chaisuwan, W., Phimolsiripol, Y., Chaiyaso, T., Techapun, C., Leksawasdi, N., Jantanasakulwong, K., Rachtanapun, P., Wangtueai, S., Sommano, S. R., You, S. G., Regenstein, J. M., Barba, F. J., & Seesuriyachan, P. (2021). The antiviral activity of bacterial, fungal, and algal polysaccharides as bioactive ingredients: potential uses for enhancing immune systems and preventing viruses. *Frontiers in Nutrition*, 8, 772033. http://dx.doi.org/10.3389/fnut.2021.772033. PMid:34805253.

Chen, Y. C., Weng, S. W., Ding, J. Y., Lee, C. H., Ku, C. L., Huang, W. C., You, H. L., & Huang, W. T. (2015). Clinicopathological manifestations and immune phenotypes in adult-Onset immunodeficiency with anti-interferon-γ autoantibodies. *Journal of Clinical Immunology*, 42(3), 672-683. http://dx.doi.org/10.1007/s10875-022-01210-y. PMid:35089479.

Cheng, J., Song, J., Liu, Y., Lu, N., Wang, Y., Hu, C., He, L., Wei, H., Lv, G., Yang, S., & Zhang, Z. (2020). Conformational properties and biological activities of α- D-mannan from *Sanghuangporus sanghuang* in liquid culture. *International Journal of Biological Macromolecules*, 164, 3568-3579. http://dx.doi.org/10.1016/j.ijbiomac.2020.08.112. PMid:32810532.

Cluff, E., Magdaleno, C. C., Fernandez, E., House, T., Swaminathan, S., Varadaraj, A., & Rajasekaran, N. (2022). Hypoxia-inducible factor-1 alpha expression is induced by IL-2 via the PI3K/mTOR pathway in hypoxic NK cells and supports effector functions in NKL cells and ex vivo expanded NK cells. *Cancer Immunology, Immunotherapy*, 71(8), 1989-2005. http://dx.doi.org/10.1007/s00262-021-03126-9. PMid:34999917.

Cui, Y., Chen, Y., Wang, S., Wang, S., Yang, J., Ismael, M., Wang, X., & Lü, X. (2023). Purification, structural characterization and antioxidant activities of two neutral polysaccharides from persimmon peel. *International Journal of Biological Macromolecules*, 225, 241-254. http://dx.doi.org/10.1016/j.ijbiomac.2022.10.257. PMid:36332822.

Duan, Z., Zhang, Y., Zhu, C., Wu, Y., Du, B., & Ji, H. (2020). Structural characterization of phosphorylated *Pleurotus ostreatus* polysaccharide and its hepatoprotective effect on carbon tetrachloride-induced liver injury in mice. *International Journal of Biological Macromolecules*, 162, 533-547. http://dx.doi.org/10.1016/j.ijbiomac.2020.06.107. PMid:32565302.

Eissa, M. A., Hashim, Y. Z. H., Abdul Azziz, S. S. S., Salleh, H. M., Isa, M. L. M., Abd Warif, N. M., Abdullah, F., Ramadan, E., & El-Kersh, D. M. (2022). Phytochemical Constituents of *Aquilaria malaccensis* leaf extract and their anti-inflammatory activity against LPS/IFN-γ-stimulated RAW 264.7 cell line. *ACS Omega*, 7(18), 15637-15646. http://dx.doi.org/10.1021/acsomega.2c00439. PMid:35571776.

El-Naggar, N. E. A., Hussein, M. H., Shaaban-Dessuuki, S. A., & Dalal, S. R. (2020). Production, extraction, and characterization of

Chlorella vulgaris soluble polysaccharides and their applications in AgNPs biosynthesis and biostimulation of plant growth. *Scientific Reports*, 10(1), 3011. http://dx.doi.org/10.1038/s41598-020-59945-w. PMid:32080302.

Ernst, L., Werner, A., & Wefers, D.. (2023). Influence of ultrasonication and hydrolysis conditions in methylation analysis of bacterial homoexopolysaccharides. *Carbohydrate Polymers*, 308, 120643. http://dx.doi.org/10.1016/j.carbpol.2023.120643. PMid:36813336.

Espinosa Gonzalez, M., Volk-Draper, L., Bhattarai, N., Wilber, A., & Ran, S. (2022). Th2 cytokines IL-4, IL-13, and IL-10 promote differentiation of pro-lymphatic progenitors derived from bone marrow myeloid precursors. *Stem Cells and Development*, 31(11-12), 322-333. http://dx.doi.org/10.1089/scd.2022.0004. PMid:35442077.

Fatmi, S., Bagati, K., Dutta, S., & Sharma, J. (2022). Characterisation of seriousness and outcome of adverse drug reactions in patients received cancer chemotherapy drugs: a prospective observational study. *Current Medicine Research and Practice*, 12(1), 20-25. http://dx.doi.org/10.4103/cmrp.cmrp_107_21.

Ganesan, K., & Xu, B. (2019). Anti-diabetic effects and mechanisms of dietary polysaccharides. *Molecules*, 24(14), 2556. http://dx.doi.org/10.3390/molecules24142556. PMid:31337059.

Gao, M. G., & Zhao, X. S. (2022). Mining the multifunction of mucosal-associated invariant T cells in hematological malignancies and transplantation immunity: a promising hexagon soldier in immunomodulatory. *Frontiers in Immunology*, 13, 931764. http://dx.doi.org/10.3389/fimmu.2022.931764. PMid:36052080.

Guo, C. L., Guo, D. D., Fang, L., Sang, T. T., Wu, J. J., Guo, C. J., Wang, Y. J., Wang, Y., Chen, C. J., Chen, J. J., Chen, R., & Wang, X. Y. (2021). *Ganoderma lucidum* polysaccharide modulates gut microbiota and immune cell function to inhibit inflammation and tumorigenesis in colon. *Carbohydrate Polymers*, 267, 118231. http://dx.doi.org/10.1016/j.carbpol.2021.118231. PMid:34119183.

Han, C., Wang, Y., Liu, R., Ran, B., & Li, W. (2022). Structural characterization and protective effect of *Lonicerae flos* polysaccharide on cyclophosphamide-induced immunosuppression in mice. *Ecotoxicology and Environmental Safety*, 230, 113174. http://dx.doi.org/10.1016/j.ecoenv.2022.113174. PMid:34999342.

Hassan, H. M., Mahran, Y. F., & Ghanim, A. M. H. (2021). *Ganoderma lucidum* ameliorates the diabetic nephropathy via down-regulatory effect on TGFβ-1 and TLR-4/NFκB signalling pathways. *The Journal of Pharmacy and Pharmacology*, 73(9), 1250-1261. http://dx.doi.org/10.1093/jpp/rgab058. PMid:33847358.

Hu, C., Li, H. X., Zhang, M. T., & Liu, L. F. (2020). Structure characterization and anticoagulant activity of a novel polysaccharide from *Leonurus artemisia* (Laur.). *RSC Advances*, 10(4), 2254-2266. http://dx.doi.org/10.1039/C9RA10853J. PMid:35494573.

Isakov, N., & Altman, A. (1986). Lymphocyte activation and immune regulation. *Immunology Today*, 7(6), 155-157. http://dx.doi.org/10.1016/0167-5699(86)90156-8.

Ito, K., Hirao, A., Arai, F., Takubo, K., Matsuoka, S., Miyamoto, K., Ohmura, M., Naka, K., Hosokawa, K., Ikeda, Y., & Suda, T. (2006). Reactive oxygen species act through p38 MAPK to limit the lifespan of hematopoietic stem cells. *Nature Medicine*, 12(4), 446-451. http://dx.doi.org/10.1038/nm1388. PMid:16565722.

Jenkinson, E., Kingston, R., & Owen, J. (1987). Importance of IL-2 receptors in intra-thymic generation of cells expressing T-cell receptors. *Nature*, 329(6135), 160-162. http://dx.doi.org/10.1038/329160a0. PMid:3114642.

Ji, X., Hou, C., Yan, Y., Shi, M., & Liu, Y. (2020). Comparison of structural characterization and antioxidant activity of polysaccharides from jujube (*ziziphus jujuba* mill.) fruit. *International Journal of Biological Macromolecules*, 149, 1008-1018. http://dx.doi.org/10.1016/j.ijbiomac.2020.02.018. PMid:32032709.

Ji, X., Liu, F., Peng, Q., & Wang, M. (2018). Purification, structural characterization, and hypolipidemic effects of a neutral polysaccharide from *Ziziphus Jujuba cv. Muzao. Food Chemistry*, 245, 1124-1130. http://dx.doi.org/10.1016/j.foodchem.2017.11.058. PMid:29287331.

Jiang, M. H., Zhu, L., & Jiang, J. G. (2010). Immunoregulatory actions of polysaccharides from Chinese herbal medicine. *Expert Opinion on Therapeutic Targets*, 14(12), 1367-1402. http://dx.doi.org/10.1517/14728222.2010.531010. PMid:21058924.

Khajepour, F., Zangouyee, M. R., Khosravimashizi, A., Afgar, A., Abdollahi, V., Dabiri, S., & Nosratabadi, R. (2022). Caraway extract alleviates atopic dermatitis by regulating oxidative stress, suppressing Th2 cells, and upregulating Th1 cells in mice. *Asian Pacific Journal of Tropical Biomedicine*, 12(10), 421-429. http://dx.doi.org/10.4103/2221-1691.357741.

Kim, H., Kwak, B. S., Hong, H. D., Suh, H. J., & Shin, K. S. (2016). Structural features of immunostimulatory polysaccharide purified from pectinase hydrolysate of barley leaf. *International Journal of Biological Macromolecules*, 87, 308-316. http://dx.doi.org/10.1016/j.ijbiomac.2016.02.072. PMid:26944661.

Le, T. H., Le, L. S., Nguyen, D. G. C., Tran, T. V. T., Vu Ho, X. A., Tran, T. M., Nguyen, M. N., Nguyen, V. T., Le, T. T., Nguyen, T. H. C., Nguyen, C. C., & Le, Q. V. (2022). Rich d-Fructose-containing polysaccharide isolated from *Myxopyrum smilacifolium* roots toward a superior antioxidant biomaterial. *ACS Omega*, 7(51), 47923-47932. http://dx.doi.org/10.1021/acsomega.2c05779. PMid:36591194.

Liang, X., Gao, Y., Pan, Y., Zou, Y., He, M., He, C., Li, L., Yin, Z., & Lv, C. (2019). Purification, chemical characterization, and antioxidant activities of polysaccharides isolated from *Mycena dendrobii*. *Carbohydrate Polymers*, 203, 45-51. http://dx.doi.org/10.1016/j.carbpol.2018.09.046. PMid:30318234.

Liu, H., Zhuang, S., Liang, C., He, J., Brennan, C. S., Brennan, M. A., Ma, L., Xiao, G., Chen, H., & Wan, S. (2022). Effects of a polysaccharide extract from Amomum villosum Lour. on gastric mucosal injury and its potential underlying mechanism. *Carbohydrate Polymers*, 294, 119822. http://dx.doi.org/10.1016/j.carbpol.2022.119822. PMid:35868771.

McConnell, B. O., & Antoniewicz, M. R. (2016). Measuring the composition and stable-isotope labeling of algal biomass carbohydrates via gas chromatography/mass spectrometry. *Analytical Chemistry*, 88(9), 4624-4628. http://dx.doi.org/10.1021/acs.analchem.6b00779. PMid:27042946.

Meng, X., Liang, H., & Luo, L. (2017). Antitumor polysaccharides from mushrooms: a review on the structural characteristics, antitumor mechanisms and immunomodulating activities. *Carbohydrate Research*, 424, 30-40. http://dx.doi.org/10.1016/j.carres.2016.02.008. PMid:26974354.

Miura, T., Kubo, M., Itoh, Y., Iwamoto, N., Kato, M., Park, S. R., Ukawa, Y., Kita, Y., & Suzuki, I. (2002). Antidiabetic activity of *Lyophyllum decastes* in genetically type 2 diabetic mice. *Biological & Pharmaceutical Bulletin*, 25(9), 1234-1237. http://dx.doi.org/10.1248/bpb.25.1234. PMid:12230127.

Mohammed, M. J., Tadros, M. G., & Michel, H. E. (2020). Geraniol protects against cyclophosphamide-induced hepatotoxicity in rats: possible role of MAPK and PPAR-gamma signaling pathways. *Food and Chemical Toxicology*, 139, 111251. http://dx.doi.org/10.1016/j.fct.2020.111251. PMid:32171873.

Nakamura, T., Itokawa, Y., Tajima, M., Ukawa, Y., Cho, K. H., Choi, J. S., Ishid, T., & Gu, Y. (2007). Radioprotective effect of *Lyophyllum*

decastes and the effect on immunological functions in irradiated mice. *Journal of Traditional Chinese Medicine*, 27(1), 70-75. PMid:17393633.

Qiu, S. M., Aweya, J. J., Liu, X. J., Liu, Y., Tang, S. J., Zhang, W. C., & Cheong, K. L. (2022). Bioactive polysaccharides from red seaweed as potent food supplements: a systematic review of their extraction, purification, and biological activities. *Carbohydrate Polymers*, 275, 118696. http://dx.doi.org/10.1016/j.carbpol.2021.118696. PMid:34742423.

Raman, M., Chen, W., & Cobb, M. H. (2007). Differential regulation and properties of MAPKs. *Oncogene*, 26(22), 3100-3112. http://dx.doi.org/10.1038/sj.onc.1210392. PMid:17496909.

Ramberg, G. E., Nelson, E. D., & Sinnott, R. A. (2010). Immunomodulatory dietary polysaccharides: a systematic review of the literature. *Nutrition Journal*, 9(1), 54. http://dx.doi.org/10.1186/1475-2891-9-54. PMid:21087484.

Roberts, C. J., Nelson, B., Marton, M. J., Stoughton, R., Meyer, M. R., Bennett, H. A., He, Y. D., Dai, H., Walker, W. L., Hughes, T. R., Tyers, M., Boone, C., & Friend, S. H. (2000). Signaling and circuitry of multiple MAPK pathways revealed by a matrix of global gene expression profiles. *Science*, 287(5454), 873-880. http://dx.doi.org/10.1126/science.287.5454.873. PMid:10657304.

Roszczyk, A., Zych, M., Zielniok, K., Krata, N., Turło, J., Klimaszewska, M., Zagożdżon, R., & Kaleta, B. (2022). The effect of novel selenopolysaccharide isolated from lentinula edodes mycelium on human T lymphocytes activation, proliferation, and cytokines synthesis. *Biomolecules*, 12(12), 1900. http://dx.doi.org/10.3390/biom12121900. PMid:36551328.

Serre, K., Mohr, E., Gaspal, F., Lane, P. J., Bird, R., Cunningham, A. F., & Maclennan, I. C. (2010). IL-4 directs both CD4 and CD8 T cells to produce Th2 cytokines *in vitro*, but only CD4 T cells produce these cytokines in response to alum-precipitated protein in vivo. *Molecular Immunology*, 47(10), 1914-1922. http://dx.doi.org/10.1016/j.molimm.2010.03.010. PMid:20392496.

Shardina, K. Y., Timganova, V. P., Bochkova, M. S., Khramtsov, P. V., Rayev, M. B., & Zamorina, S. A. (2022). The role of recombinant glycodelin in the differentiation of regulatory t-lymphocytes. *Doklady Biological Sciences*, 506(1), 137-140. http://dx.doi.org/10.1134/S0012496622050131. PMid:36301420.

Song, Y., Zhu, M., Hao, H., Deng, J., Li, M., Sun, Y., Yang, R., Wang, H., & Huang, R. (2019). Structure characterization of a novel polysaccharide from Chinese wild fruits (*Passiflora foetida*) and its immune-enhancing activity. *International Journal of Biological Macromolecules*, 136, 324-331. http://dx.doi.org/10.1016/j.ijbiomac.2019.06.090. PMid:31202849.

Tian, Y., Zhao, Y., Zeng, H., Zhang, Y., & Zheng, B. (2016). Structural characterization of a novel neutral polysaccharide from *Lentinus giganteus* and its antitumor activity through inducing apoptosis. *Carbohydrate Polymers*, 154, 231-240. http://dx.doi.org/10.1016/j.carbpol.2016.08.059. PMid:27577914.

Trache, A., & Meininger, G. A. (2008). Atomic force microscopy (AFM). *Current Protocols in Microbiology*, 2, 2.1-2.17. http://dx.doi.org/10.1002/9780471729259.mc02c02s8.

Ukawa, Y., Andou, M., Furuichi, Y., Kokean, Y., Nishii, T., & Hisamatsu, M. (2001). Hypocholesterolemic activity of hatakeshimeji (*Lyophyllum decastes* sing.) mushroom in rats. *Nippon Shokuhin Kagaku Kogaku Kaishi*, 48(7), 520-525. http://dx.doi.org/10.3136/nskkk.48.520.

Ukawa, Y., Furuichi, Y., Kokean, Y., Nishii, T., & Hisamatsu, M. (2002). Effect of hatakeshimeji (*Lyophyllum decastes* Sing.) mushroom on serum lipid levels in rats. *Journal of Nutritional Science and Vitaminology*, 48(1), 73-76. http://dx.doi.org/10.3177/jnsv.48.73. PMid:12026194.

Ukawa, Y., Ito, H., & Hisamatsu, M. (2000). Antitumor effects of (1→3)-βD-glucan and (1→6)-β-glucan purified from newly cultivated mushroom, Hatakeshimeji (*Lyophyllum decastes* Sing.). *Journal of Bioscience and Bioengineering*, 90(1), 98-104. http://dx.doi.org/10.1016/S1389-1723(00)80041-9. PMid:16232825.

University of Georgia – UGA. (2022). *Complex Carbohydrate Research Center (CCRC) spectral database.* Retrieved from https://www.ccrc.uga.edu/specdb/ms/pmaa/pframe.html

Wang, W. X., & Liu, J. J. (2020). Efficient extraction, antioxidant activities and antiinflammation of polysaccharides from *Notopterygium franchetii Boiss*. *Carbohydrate Polymers*, 248, 116783. http://dx.doi.org/10.1016/j.carbpol.2020.116783. PMid:32919571.

Wang, W., Tan, J., Nima, L., Sang, Y., Cai, X., & Xue, H. (2022). Polysaccharides from fungi: a review on their extraction, purification, structural features, and biological activities. *Food Chemistry: X*, 15, 100414. http://dx.doi.org/10.1016/j.fochx.2022.100414. PMid:36211789.

Wei, S. Y., Wu, T. T., Huang, J. Q., Kang, Z. P., Wang, M. X., Zhong, Y. B., Ge, W., Zhou, B. G., Zhao, H. M., Wang, H. Y., & Liu, D. Y. (2022). Curcumin alleviates experimental colitis *via* a potential mechanism involving memory B cells and Bcl-6-Syk-BLNK signaling. *World Journal of Gastroenterology*, 28(40), 5865-5880. http://dx.doi.org/10.3748/wjg.v28.i40.5865. PMid:36353208.

Yan, J. K., Wang, W. Q., & Wu, J. Y. (2014). Recent advances in *Cordyceps Sinensis* polysaccharides: mycelial fermentation, isolation, structure, and bioactivities: a review. *Journal of Functional Foods*, 6, 33-47. http://dx.doi.org/10.1016/j.jff.2013.11.024. PMid:32362940.

Yin, Z. H., Liang, Z. H., Li, C. Q., Wang, J. M., Ma, C. Y., & Kang, W. Y. (2021). Immunomodulatory effects of polysaccharides from edible fungus: a review. *Food Science and Human Wellness*, 10(4), 393-400. http://dx.doi.org/10.1016/j.fshw.2021.04.001.

Yun, D., Yan, Y., & Liu, J. (2022). Isolation, structure and biological activity of polysaccharides from the fruits of *Lycium ruthenicum* Murr: a review. Carbohydrate Polymers, 291, 119618. http://dx.doi.org/10.1016/j.carbpol.2022.119618. PMid:35698413.

Zhang, F. P., Xu, H., Yuan, Y., Huang, H. C., Wu, X. P., Zhang, J. L., & Fu, J. S. (2022). *Lyophyllum decastes* fruiting body polysaccharide alleviates acute liver injury by activating the Nrf2 signaling pathway. *Food & Function*, 13(4), 2057-2067. http://dx.doi.org/10.1039/D1FO01701B. PMid:35107114.

Zhang, W. B., Zhang, H. Y., Jiao, F. Z., Wang, L. W., Zhang, H., & Gong, Z. J. (2018). Histone deacetylase 6 inhibitor ACY-1215 protects against experimental acute liver failure by regulating the TLR4-MAPK/NF-kappaB pathway. *Biomedicine and Pharmacotherapy*, 97, 818-824. http://dx.doi.org/10.1016/j.biopha.2017.10.103. PMid:29112935.

Zheng, Y., Zong, Z. M., Chen, S. L., Chen, A. H., & Wei, X. Y. (2017). Ameliorative effect of *Trametes orientalis* polysaccharide against immunosuppression and oxidative stress in cyclophosphamide-treated mice. *International Journal of Biological Macromolecules*, 95, 1216-1222. http://dx.doi.org/10.1016/j.ijbiomac.2016.11.013. PMid:27825995.